http://dx.doi.org/10.5012/bkcs.2012.33.5.1491

InP Quantum Dot-Organosilicon Nanocomposites

Mai Xuan Dung, Priyaranjan Mohapatra, Jin-Kyu Choi, Jin-Hyeok Kim,† Sohee Jeong,‡ and Hyun-Dam Jeong*

*Department of Chemistry, Chonnam National University, Gwangju 500-757, Korea. *E-mail: hdjeong@chonnam.ac.kr*
†Department of Material Science and Engineering, Chonnam National University, Gwangju 500-757, Korea
‡Nanomechanical Systems Research Division, Korea Institute of Machinery and Materials, Daejeon 305-343, Korea
Received October 22, 2011, Accepted February 1, 2012

InP quantum dot (QD)-organosilicon nanocomposites were synthesized and their photoluminescence quenching was mainly investigated because of their applicability to white LEDs (light emitting diodes). The as-synthesized InP QDs are capped with myristic acid (MA), which are incompatible with typical silicone encapsulants. We have introduced a new ligand, 3-aminopropyldimethylsilane (APDMS), which enables embedding the QDs into vinyl-functionalized silicones through direct chemical bonding. The exchange of ligand from MA to APDMS does not significantly affect the UV absorbance of the InP QDs, but quenches the PL to about 10% of its original value with the relative increase in surface related emission intensities, which is explained by stronger coordination of the APDMS ligands to the surface indium atoms. InP QD-organosilicon nanocomposites were synthesized by connecting the QDs using a short cross-linker such as 1,4-divinyl-tetramethylsilylethane (DVMSE) by the hydrosilylation reaction. The formation and changes in the optical properties of the InP QD-organosilicon nanocomposite were monitored by ultraviolet visible (UV-vis) absorbance and steady state photoluminescence (PL) spectroscopies. As the hydrosilylation reaction proceeds, the QD-organosilicon nanocomposite is formed and grows in size, causing an increase in the UV-vis absorbance due to the scattering effect. At the same time, the PL spectrum is red-shifted and, very interestingly, the PL is quenched gradually. Three PL quenching mechanisms are regarded as strong candidates for the PL quenching of the QD nanocomposites, namely the scattering effect, Förster resonance energy transfer (FRET) and cross-linker tension preventing the QD's surface relaxation.

Key Words : InP quantum dot, Organosilicon, Nanocomposite, PL quenching, Ligand exchange

Introduction

A semiconductor quantum dot (QD) is a nano-sized, crystalline particle consisting of hundreds to thousands of atoms, falling in the gap between molecular cluster and bulk crystal.[1a] The energy gap of quantum dot is approximately proportional to $1/R^2$ (where R is its radius), giving rise to a tunable emission color and absorption onset in a wide range. Since electron - hole pairs can be created in the QDs by carrier injection or by the photoexcitation, QDs can be utilized as light emitter or wavelength down converting materials, respectively, in light emitting devices.[1b]

Well established synthesis procedures are now available to provide a variety of QDs with high quality, *viz.* a narrow size distribution, tunable and pure emission color, and high quantum yield.[2,3] Especially, suppressed or even non-blinking QDs have also been demonstrated.[4] Thanks to these developments, the QDs are expected to be good wavelength converting materials for white light emitting diode (white-LED) applications. Most of the commercially available white-LEDs are down conversion LEDs which contain one LED chip emitting luminous blue light and an additional yellow phosphor (Ce-doped YAG) embedded in an encapsulant, as depicted in Figure 1(a).[5] Two issues need resolving to improve the performance of the current white-LEDs, namely, thermal degradation of the encapsulant and the quality of the white light. As regards the first issue, the traditional encapsulants based on epoxy polymers become yellow and lose their transparency gradually during their exposure to light irradiation and operation at high temperatures, usually above 120 °C.[6a] Therefore, silicones have been preferred as the LED encapsulants because of their high thermal and UV stabilities originating from the siloxane backbones. However, limitation of using the silicone encapsulants is their low refractive indices compared to those of epoxy polymers. Most silicones have refractive indices in the range from 1.40 to 1.55 whereas those of epoxy polymers are high as 1.62.[6b] In our recent study investigating the refractive index tunability of silsexquioxane thin films made from methyltrimethoxysilane (MTMS) and 4,4'-bis-(trimethoxysilylmethyl)biphenyl (MBP), we pointed out that the high refractive index is afforded by the aromatic groups containing a π-electron cloud in the films.[6c] A refractive index of 1.60 was achieved in the silsesquioxane thin film made using the 100% MBP condition. Accordingly, we concluded that the first issue can be resolved by using silicones including aromatic groups as the encapsulant materials.

The second issue is the lack of the green and red bands in the emission spectrum of the white-LEDs, perceived due to the yellow YAG:Ce phosphor, as depicted in Figure 1(b). To improve the white light quality we designed red emitting InP QDs to be used as supplemental phosphor to the yellow

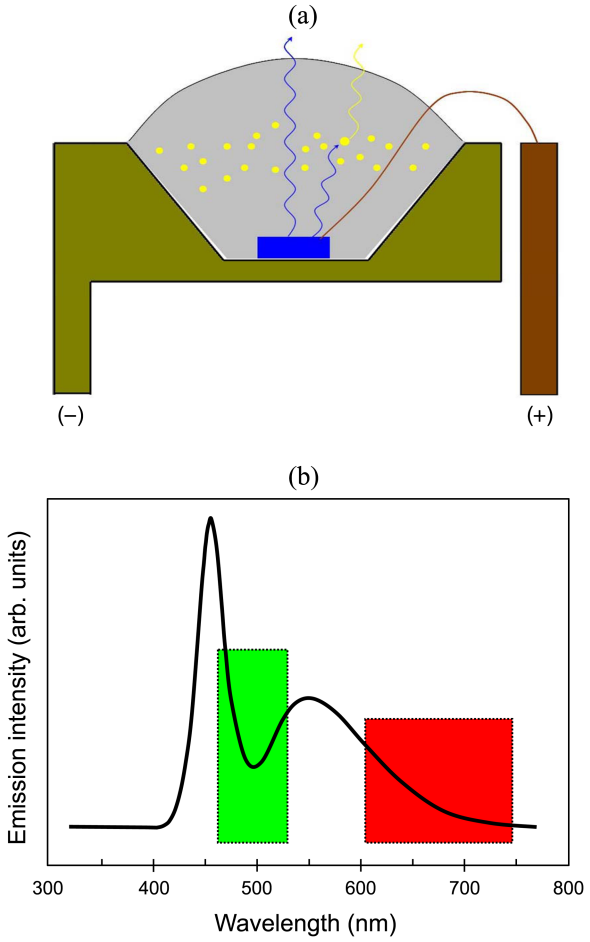

Figure 1. (a) Structure of the down conversion white LED: The yellow phosphor Ce:YAG dispersed in the encapsulant partially converts the luminous blue light from the blue chip to yellow light. (b) Emission spectrum of a down conversion white LED using the yellow Ce:YAG phosphor. The lack of the green and red band emission perceived originated from the Ce:YAG phosphor accounts for its poor white light quality.

YAG:Ce phosphor. The InP QDs were chosen because 1) they have less toxicity than the typical II-VI QDs containing Cd or Se elements; 2) high quantum yield (60-70%) can be achieved,[2f] giving rise to a high wavelength conversion efficiency; and 3) they also provide tunable emission color in the visible range.[2a] During the development of QD phosphor, we revealed that, in addition to the quantum efficiency and the emission color, chemical interaction between the QDs and the silicone encapsulant is very important for their miscibility. This discovery led to an innovation in improving the compatibility of the QD-silicone system, wherein the QDs are chemically interconnected to vinyl-functionalized silicone by using hydrosilylation reaction. The stepwise innovation process is summarized in Scheme 1.

The myristic acid capped InP QDs (abbreviated as InP-MA) are incompatible with the commercial silicon encapsulant, Dow Corning 6630B, owing to the large difference in their Hansen's solubility parameters.[7a] Recapping of InP-MA QDs with 3-aminopropyltrimethoxysilane (APTMS) was expected to gain QDs having the Si-OCH_3 groups on the

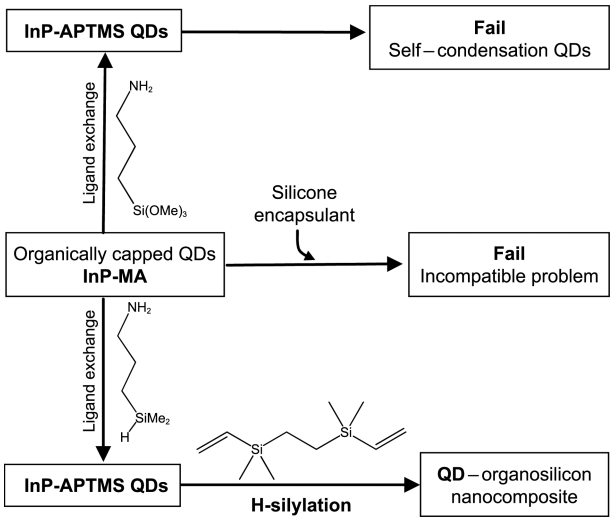

Scheme 1. Innovative development of QD-organosilicon materials wherein QDs are chemically bonded directly to a vinyl-functionalized organosilicon compound.

surface, (abbreviated by InP-APTMS), which may enable combining the QDs with various alkoxysilanes relying the sol-gel approach. However, the resultant QDs was not soluble in various solvents, presumably due to the self-condensation between the InP-APTMS QDs during the ligand exchange and/or purification steps. To overcome these problems, we have introduced a new ligand, 3-aminopropyldimethylsilane (APDMS), which has the amino group (-NH_2) at one end to be coordinated to the QD surface and a silane (Si-H) group at the other end, as shown in Scheme 1. Since the QDs obtained after ligand exchanging with the APDMS (abbreviated by InP-APDMS) bearing Si-H groups on their surface cannot react between themselves. In addition, the InP-APDMS QDs can be bonded to various vinyl-functionalized silicones through the hydrosilylation reaction, as illustrated in Scheme 2. In this way, the above aggregation and self-condensation problems are expected to

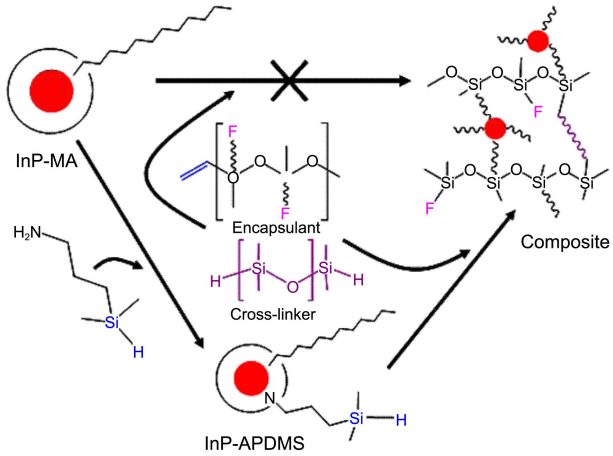

Scheme 2. The direct chemical bonding of the QD phosphor to the silicone encapsulant is made possible by using the APDMS ligand. F is a group which allows the physical properties to be controlled, such as phenyl or methyl.

be prevented. The photoluminescence (PL) quenching after the ligand exchange was observed, and its physical-chemical origin was investigated from cluster model calculations using DFT-B3LYP level

In this article, the syntheses and optical characterizations of the InP (InP/ZnS) QD-organosilicon nanocomposite materials were also performed, in order to 1) investigate the origin of the physico-chemical interaction between the QDs which affects their optical properties and 2) design a basic process architecture for dispersing the QDs as a phosphor into the silicone encapsulants containing a vinyl-terminated silicone monomer for the white LED device.

The syntheses of the QD-organosilicon nanocomposite materials were performed by forming direct chemical bonding, where the QDs bearing silylable -Si-H groups on their surface are cross-linked by 1,4-divinyltetramethyldisilylethane (DVMSE) molecules using the hydrosilylation reaction. The interactions between the QDs in the nanocomposites were investigated by using ultraviolet visible (UV-vis) absorbance and steady state photoluminescence (PL) spectroscopies. As the size of the QD-organosilicon nanocomposite increases, as confirmed by the change in its UV-vis absorbance in toluene solution based on the scattering effect, its PL spectrum is red-shifted and, very interestingly, its intensity is quenched simultaneously. We consider four possible mechanisms which could explain the PL quenching in the QD-organosilicon composite, namely the scattering effect, Förster resonance energy transfer (FRET), cross-linker tension preventing the QD's surface relaxation, and photo-induced charge transfer from one QD to another.

Experimental Section

Synthesis of Myristic Acid Capped InP (InP-MA) and InP/ZnS Core-Shell (InP/ZnS-MA) Quantum Dots. The InP-MA QDs were synthesized by the procedure reported by Battaglia.[2b] Briefly, an indium solution consisting of 0.62 mmol indium acetate, 2.11 mmol myristic acid (MA) and 32 mL of technical grade octadecene (ODE) (Sigma-Aldrich, St. Louis, MO, USA) was degassed at 120 °C for 2 hours under vacuum. The solution was then refilled with argon gas and quickly heated to 300 °C. When the temperature was stable at 300 °C, 6 mL of a phosphine solution containing 0.31 mmol tris(trimethylsilyl)phosphine (JSI Silicone Co. Ltd., Seongnam, South Korea) in ODE was rapidly injected. The injection quenched the reaction temperature to 278 °C, which was controlled constantly for 20 minutes by adjusting the heating mantle. The resultant solution was quickly cooled to room temperature to perform the InP-MA QD or to about 150 °C for the post-shelling with ZnS.

To synthesize the InP/ZnS-MA QDs, we adopted the procedure reported by Peng[2a] with a small change; *viz.* zinc acetate (Alfa Aesar, 99.98%) was used instead of zinc stearate. Two separate solutions of zinc acetate and sulfur (Aldrich, 99.998%) at concentrations of 0.1 M in ODE were prepared and pre-heated to 110 °C under Ar gas flow. For the first ZnS layer, 2 mL each of these solutions was injected into the as-prepared InP QDs solution at 150 °C in succession at 20 minute intervals. The reaction mixture was then heated to 230 °C and kept at this temperature for 1 hour to grow the first ZnS layer. This procedure was repeated for the deposition of the second ZnS layer, but 2.9 mL each of the Zn and S precursor solutions were used.

After cooling down the InP, InP/ZnS-MA QDs solutions to room temperature, an equivalent volume of hexane (co-solvent) (about 40 mL) was added. Acetone (non-solvent) was added to precipitate the QDs which were then collected by centrifugation at speed of 10,000 rotations per minute (rpm) for 10 minutes and re-dispersed again in hexane. This hexane-acetone purification cycle was repeated for at least two times. QDs were then stored in anhydrous hexane in a dark container. Before being used for the ligand exchange reactions, these QDs were purified one time with methylenechloride-acetone. This step was conducted in order to completely remove the impurities such as hentriacontan-16-one and ODE which remained after the hexane-acetone purification procedure.[8]

Ligand Exchange.

Ligand Exchange with 3-Aminopropyltrimethoxysilane (APTMS). 0.2 mL APTMS (97%, Aldrich) was added to 10 mL of a MC solution (C_M about 2.5×10^{-6} M as estimated from UV absorbance) of the InP-MA QDs under stirring. After 8 hours, the InP-APTMS QDs was precipitated by adding n-hexane and collected by centrifugation at 5000 rotations per minute (rpm) for 10 minutes. However, the collected InP-APTMS QDs were not soluble in any solvents of interest, including MC, toluene, tetrahydrofuran, ethanol, methanol and acetonitrile. To understand this gelation, a drop of the MC solution prior to hexane addition was dried on a TEM copper grid under the ambient conditions. The TEM picture is shown in Figure 3(b).

Ligand Exchange with 3-Aminopropyldimethylsilane (APDMS): 3-Aminopropyldimethylsilane (APDMS) was designed by our laboratory, synthesized and supplied by JSI Silicone Co. Ltd. (Seongnam, South Korea). The detailed synthesis procedure and analyses including GC-MAS (Figure S1a) and ^{1}H-NMR (Figure S1b) spectroscopies of the APDMS ligand are contained in the supporting information. The product contains 30 molar percent of a side-product (2,2-dimethyl-1,2-azasilolidine), as deduced from the ^{1}H-NMR spectrum, Figure S1b. For the ligand exchange reaction, 0.2 mL of the APDMS was added to 20 mL of a MC solution (C_M = 5.7 μM as estimated from UV absorbance) of the InP-MA or InP/ZnS-MA under stirring at 40 °C. After 5 hours, the AMDPS capped QDs were precipitated with acetonitrile and collected by centrifugation.

Synthesis of InP and InP/ZnS QD-Organosilicon Nanocomposites. 0.044 g of the InP-APDMS QDs (or 0.040 g of InP/ZnS-APDMS QDs), 0.6 g of 1,4-divinyltetramethylsilylethane (DVMSE) and 30 mL of toluene were added to a 100 mL flask, which was connected to a Schlenk line system and a heat controller. 0.3 mL of Karstedt catalyst solution (2 wt % in toluene, JSI Silicone Co. Ltd.) was then added and the reaction mixture was maintained at 60 °C. 2 mL aliquots

of the reaction solution were withdrawn from the reaction solution through a syringe after different reaction times (0, 1, 5, 10, 24, and 48 hours for InP QD-organosilicon nanocomposite; 0, 1, 2, 10, 24, 48 hours for InP/ZnS QD-organosilicon nanocomposite). During the reaction, the color was changed from red to dark red.

Characterizations. UV-vis absorbance and photoluminescence spectroscopies were employed to investigate the optical properties of QDs and QD-organosilicon nanocomposite. UV-vis absorbance spectroscopy was performed in the 200-1000 nm range with a SCINCO S-3150 spectrophotometer. Photoluminescence spectroscopy was carried out using a He-Cd (Kimmon Electric Co., IK3501R-G, Japan) light source at 325 nm with 50 mW power and a photodiode array detector (IRY1024, Princeton Instrument Co., U.S.A.). The surface properties of the QDs before and after the ligand exchange process were investigated by nuclear magnetic resonance (NMR) spectroscopy, which was performed on a superconducting FT-NMR 300MHz (Varian Inc, Palo Alto, California, U.S.A.). For the X-ray diffraction (XRD) measurements, the solution of InP-MA in MC was dropped on a piece of silicon wafer and allowed to dry. The XRD pattern was recorded in the range of two theta angles from 10° to 60° on an X'Pert PRO Multiple Purpose X-ray diffractometer (PANalytical). Transmission electron microscopy (TEM) was performed on a JEOL JEM-1400 (JEOL Ltd. Akisima, Tokyo, Japan). For sampling, dilute solutions of InP-MA in MC and InP-APDMS in MC were dropped on a copper rigid, dried and stored in a vacuum oven.

Theoretical Methods. Theoretical calculations were carried out to explain PL quenching phenomena due to the ligand exchange. All calculations were performed at DFT-B3LYP level and LANL2DZ basis set in Gaussian03 package. Details are discussed in below results and discussion section (Table 2 and Figure 8).

Results and Discussion

The UV-vis absorbance spectrum of the myristic acid capped InP QDs (InP-MA) in toluene solution, in Figure 2, shows an absorption peak centered at about 580 nm, indicating their narrow size distribution. Using the statistical relation between the QD size and the first excitonic peak position (D = 0.0133x-4.43, where D and x are the diameter of the QD and position of the first excitonic peak, respectively, in our case x = 580 nm),[9] the diameter of the InP QD is found to be about 3.3 nm. The photoluminescence (PL) spectrum of the same solution under excitation at 325 nm shows an intense peak at about 628 nm with a full width at half maximum (FWHM) of 68 nm corresponding to the band edge emission. The broad emission band at higher wavelengths, as clearly confirmed in Figure 5(b), is due to the surface related emission.[3] The crystalline nature of the InP-MA QDs are evidenced from the wide angle X-ray diffraction pattern (Supporting information, Figure S2a). Furthermore, the InP-MA QDs have zinc-blende structure because the three peaks located at 2θ = 26.4°, 43.8° and

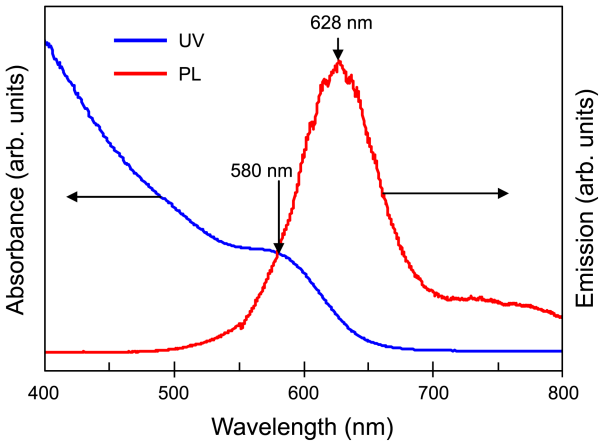

Figure 2. UV absorbance (blue line) and PL (red line) spectra of the InP-MA QDs in toluene solution.

51.8° in the XRD pattern match well with the three characteristic peaks of zinc-blende bulk InP crystal diffracted from the <111>, <220>, and <311> lattice planes, respectively.[2b] The InP-MA QDs are clearly seen in the TEM picture as black dots in the Figure S2b (Supporting information). By averaging the sizes of 30 dots observed in various TEM pictures, the diameter of the InP-MA QDs was also estimated to be about 3.6 nm.

The as-synthesized InP QDs (InP-MA) are capped with myristic acid, as mentioned earlier, is documented by comparing the ^{13}C-NMR (Supporting information, Figure S3) and ^{1}H-NMR (lower parts in the Figure 4) spectra of the InP-MA QDs and those of the myristic acid which was used as stabilizing agent in the synthesis of the QDs. The lack of three peaks corresponding to the carbon atoms in the carboxyl and the two adjacent methylene groups of the MA molecule observed in the ^{13}C-NMR spectrum of InP-MA QDs, (Supporting information, Figure S3) confirms indirectly that the MA molecules are coordinated to the surface of the InP QDs, based on the surface broadening effect. A similar observation has been reported for the InP QDs capped by palmitic acid.[8]

In our initial effort, we mixed the as-synthesized InP QDs (InP-MA) with a commercial silicone encapsulant (Dow corning 6630B) by a typical solvent mixing process (Supporting information, testing compatibility). However, the InP-MA QDs were aggregated, as clearly seen in the first row of Figure 3(a). This phase separation phenomenon is due to the difference in the solubilities of the InP-MA QDs and the silicone encapsulant. It is known that the miscibility of a solute-solvent system is governed by the similarity in their solubility. The solubility of a compound (δ_T) is composed of three Hansen's solubility parameters (HSPs), namely the dispersive interactions (δ_D), dipole-dipole interactions (δ_P) and hydrogen bonding interactions (δ_H), as expressed in Eq. (1).[7b] The more similar between the HSPs of the solute and solvent are, the more easily they mix.

$$(\delta_T)^2 = (\delta_D)^2 + (\delta_P)^2 + (\delta_H)^2 \quad (1)$$

To our knowledge, the HSPs of organically capped QDs

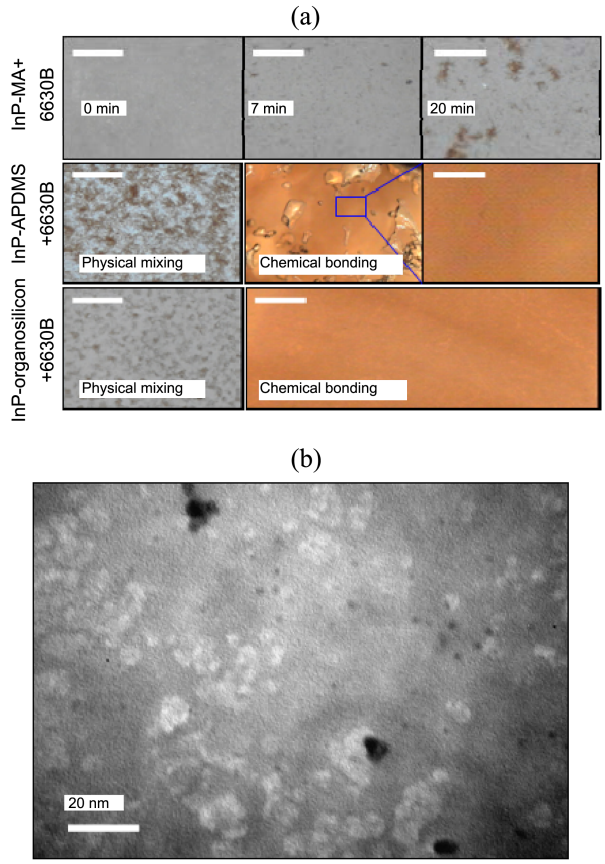

Figure 3. (a) Micrographs of InP QDs-silicone composites prepared either by physical mixing or chemical bonding methods. Top: Mixture of InP-MA QDs and silicone 6630B in toluene snapped at different time; Middle: InP-APDMS embedded in silicone 6630B by physical mixing after solvent evaporating (left) or chemical bonding using hydrosilylation (right); Bottom: the InP-DVMSE composite embedded in silicon 6630B by physical mixing (left) and obtained after hydrosilylation reaction (fight). (b) TEM picture of the InP QDs obtained by ligand exchange reaction between InP-MA QDs with 3-aminopropyltrimethoxysilane shows quantum dot aggregates together with individual dots.

such as our InP-MA QDs, have not been reported in the literature and, therefore, we used the HSPs of toluene for the InP-MA QDs in this study, since the InP-MA QDs and toluene are well miscible. The HSPs of the InP-MA QDs (represented by toluene) and various interested materials are listed in Table 1. Clearly, the poor compatibility between the InP-MA QDs (solute) and silicone encapsulant (solvent) is originated from the large difference in their hydrogen bonding interaction. The incompatible problems have been reported previously for the systems of organically capped CdSe QDs and silicones or epoxies.[7a] Without any experimental evidence, it can be additionally deduced that our InP-MA QDs may not be homogeneously dispersed in epoxy encapsulants whose dipole-dipole and hydrogen bonding interactions are much higher than that of toluene, as shown in Table 1. Post-shelling the organically capped QDs such as our InP-MA QDs with a silica shell by using a surfactant assisted sol-gel approach has been proposed to improve the compatibility.[10] However, from our view, silica obtained

Table 1. Hansen's solubility parameters (HSPs) of the materials of interest. Herein, toluene and fume silica are used to represent the InP-MA and silica coated QDs, respectively

Materials	δ_T ($MPa^{0.5}$)	δ_D ($MPa^{0.5}$)	δ_P ($MPa^{0.5}$)	δ_H ($MPa^{0.5}$)
Toluene[a]	18.2	18	1.4	2.0
Epoxies[a]	18-26	18.3	12.3	9.7
Silicones[a]	14.9-17.5	16.4	1.6	7.8
Methanol[b]	29.6	15.1	12.3	22.3
Fume silica[b*]	44	18	27.5	29
Fume silica[b]	29.6	17	19	15

[a]reference 7a. [b]reference 11. [*]when adsorbed water is considered.

from the sol-gel method such as the colloidal silica particles listed in Table 1, always have very high dipole-dipole and hydrogen bonding interactions originated from the intrinsic polarization components such as silanol (Si-OH) groups, or absorbed water.[11] When the three HSPs are considered, the silica coated QDs may not mix well with the silicone encapsulant. This argument was indirectly confirmed in our comparison experiment, which showed that the encapsulant (Dow corning 6630B) was insoluble in methanol, whose HSPs are comparable with those of fume silica, as shown in Table 1.

In order to overcome these incompatibilities that arise from the physical mixing process, phosphors which are chemically bonded to the silicone encapsulants need to be newly designed. For this purpose, we performed the exchange of ligand from MA to 3-aminopropyltrimethoxylsilane (APTMS) to obtain APTMS capped InP QDs (abbreviated by InP-APTMS). It was expected that the InP-APTMS QDs could be chemically bonded to various silicone matrix through the conventional hydrolysis-condensation reaction owing to their Si-OMe groups. However, the QDs obtained after the ligand exchange reaction were insoluble in various solvents including THF, chloroform, toluene, and even the mother solvent MC, see experimental section. To understand this gelation, a drop of the MC solution of the InP-APTMS QDs prior to hexane addition was dried on a TEM copper grid. Figure 3(b) shows QD aggregates with size of about 10 nm, corresponding to 2-4 QDs, together with the individual QDs. We assumed that InP-APTMS QDs underwent self-condensation reactions (2) and (3) forming a gel during the ligand exchange reaction or purification steps.

$$\text{QD---Si-OMe} + \text{trace } H_2O \rightarrow \text{QD---Si-OH} \quad (2)$$

$$\text{QD---Si-OH} + \text{HO-Si---QD} \rightarrow \text{QD---Si-O-Si---QD} \quad (3)$$

After considering these failures, due to the incompatible problem between the InP-MA QDs and the silicone encapsulant and the self-condensation problem with the InP-APTMS QDs, we designed a new capping ligand, namely 3-aminopropyldimethylsilane (APDMS), by means of which we can overcome both of these problems. The ligand contains hydrosilane group (Si-H), giving rise to strong chemical interactions with silicones during the encapsulating processes

in which the vinyl functionalized silicone polymers are cross-linked with hydrosilane bridges *via* hydrosilylation,[6b] as illustrated in Scheme 2. Importantly, the Si-H groups do not react with themselves, thus preventing the QDs from undergoing self-condensation. Therefore, the InP QDs capped with APDMS (abbreviated as InP-APDMS) are expected to overcome both the aggregation and self-condensation problems.

Figure 3(a) shows the microscopic pictures of various QDs-silicone encapsulant systems prepared either by physical or chemical bonding methods (Supporting information, testing the compatibility). Obviously, physical embedding the InP-MA (the top row) or InP-APDMS QDs (the middle row) into the silicone encapsulant (6630B, Dow Corning) results in the QD aggregation, whereas introducing the InP-APDMS QDs into the silicone encapsulant by chemical bonding, *via* hydrosilylation reaction, provides a homogeneous QD-silicone nanocomposite. The physical mixing between the InP QD-organosilicon nanocomposite obtained after 5 hours of hydrosilylation from the InP-APDMS and divinyltetramethylsilylethane (DVMSE) (see the experimental section) and the silicone encapsulant (Dow Corning 6630B) also results in QD rich phase separation, but a homogeneous dispersion can be obtained utilizing the same chemical mixing method, as clearly seen in the bottom row of Figure 3(a).

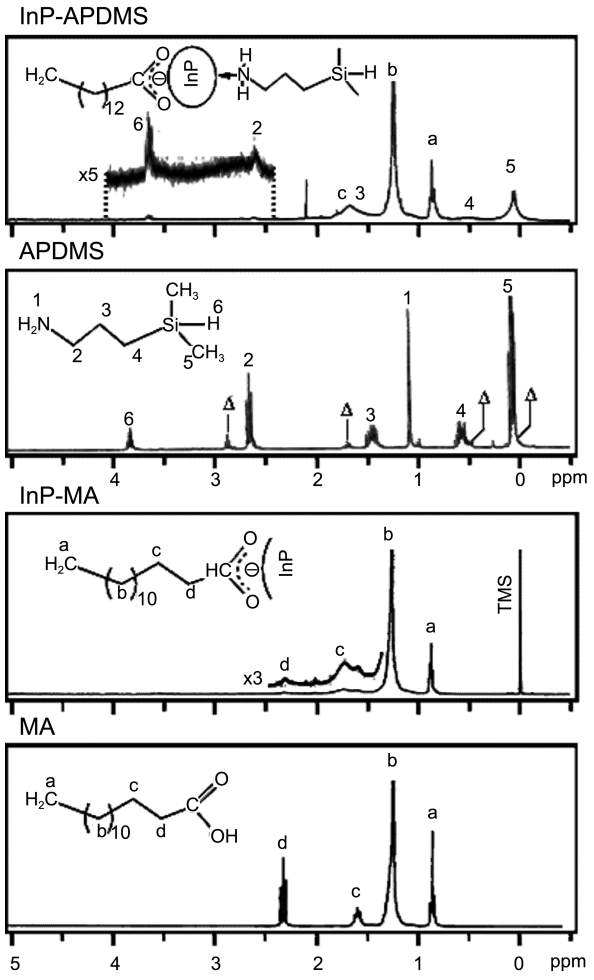

Figure 4. From bottom to top: ^{1}H-NMR spectra (in CD_2Cl_2) of myristic acid (MA); myristic acid capped InP QDs (InP-MA); 3-aminopropyldimethylsilane (APDMS) and APDMS capped InP QD (InP-APDMS). In the APDMS spectrum, the triangles (Δ) mark the peaks originating from the side product: 2,2-dimethyl-1,2-azasilolidine (supporting information, Figure S1b).

Figure 4 shows the ^{1}H-NMR spectra, respectively, of the free myristic acid (MA), the InP-MA QDs, the APDMS ligand and the InP-APDMS QDs. The similarity between the ^{1}H-NMR spectra of the MA and the InP-MA QDs supports to the previous mention that the as-synthesized InP QDs are capped by MA. The peaks of the protons **c** and **d** are broadened in the ^{1}H-NMR spectrum of the InP-MA QDs due to the surface broadening effect,[12] which also blurs the peaks of the carbon atoms adjoining to the quantum dot surface observed in the ^{13}C-NMR spectrum of InP-MA QDs (Supporting information, Figure S3). The ^{1}H-NMR spectrum of the InP-APDMS QDs, the uppermost picture in Figure 4, shows the characteristic peaks both of MA and APDMS ligands. The molar composition of the APMD on the surface of InP-APDMS QDs is estimated to be about 40% by using the integral intensities of the two well separated peaks at 0.08 ppm (assigned to proton **5** in APDMS) and 0.88 ppm (assigned to proton **a** in MA). Importantly, the ^{1}H-NMR spectrum of the InP-AMDS QDs shows an obvious peak of the proton **6** at about 3.7 ppm, indicating the presence of the Si-H groups on the surface of QDs. This peak has been shifted from 3.85 ppm (in free APDMS case). Without any experimental evidence we assume that this shift is due to the hydride head groups are weakly coordinated to the indium atoms on the surface of QDs. As expected, peak of the proton **1** (-NH_2 group in APDMS) is absent in the ^{1}H-NMR spectrum the InP-APDMS QDs, resembling to the lack of carbon peaks observed in the ^{13}C-NMR spectrum of the InP-MA QDs discussed previously, indicating that the amino groups are coordinated to the surface of QDs. Additionally, peak of proton **2'** in the side product (2,2-dimethyl-1,2-azasilolidine) at about 2.9 ppm is not observed in the ^{1}H-NMR spectrum of the InP-APDMS QDs implying that the side product was washed out.

In the typical LED packaging process, the curing step is conducted to cross-link the silicone polymers containing vinyl functional groups with the hydrosilane linkers through the hydrosilylation reaction.[6b] Therefore the InP-APDMS QDs bearing silylable groups (Si-H) on the surface can be chemically bonded to the vinyl functionalized silicone polymers in the curing step. To utilize the QDs as nanophosphor in the white LEDs, their luminescence must be maintained throughout the curing processes. Unfortunately, the quantum yield of the InP QDs is decreased by the ligand exchange process. More importantly, the PL of the QDs is further reduced when they are cross-linked in the QD-organosilicon nanocomposites. In the following sections, we will discuss mainly the PL quenching phenomena observed for both the InP and InP/ZnS QDs at the ligand exchange step and in the synthesis of the QD-organosilicone nanocomposites.

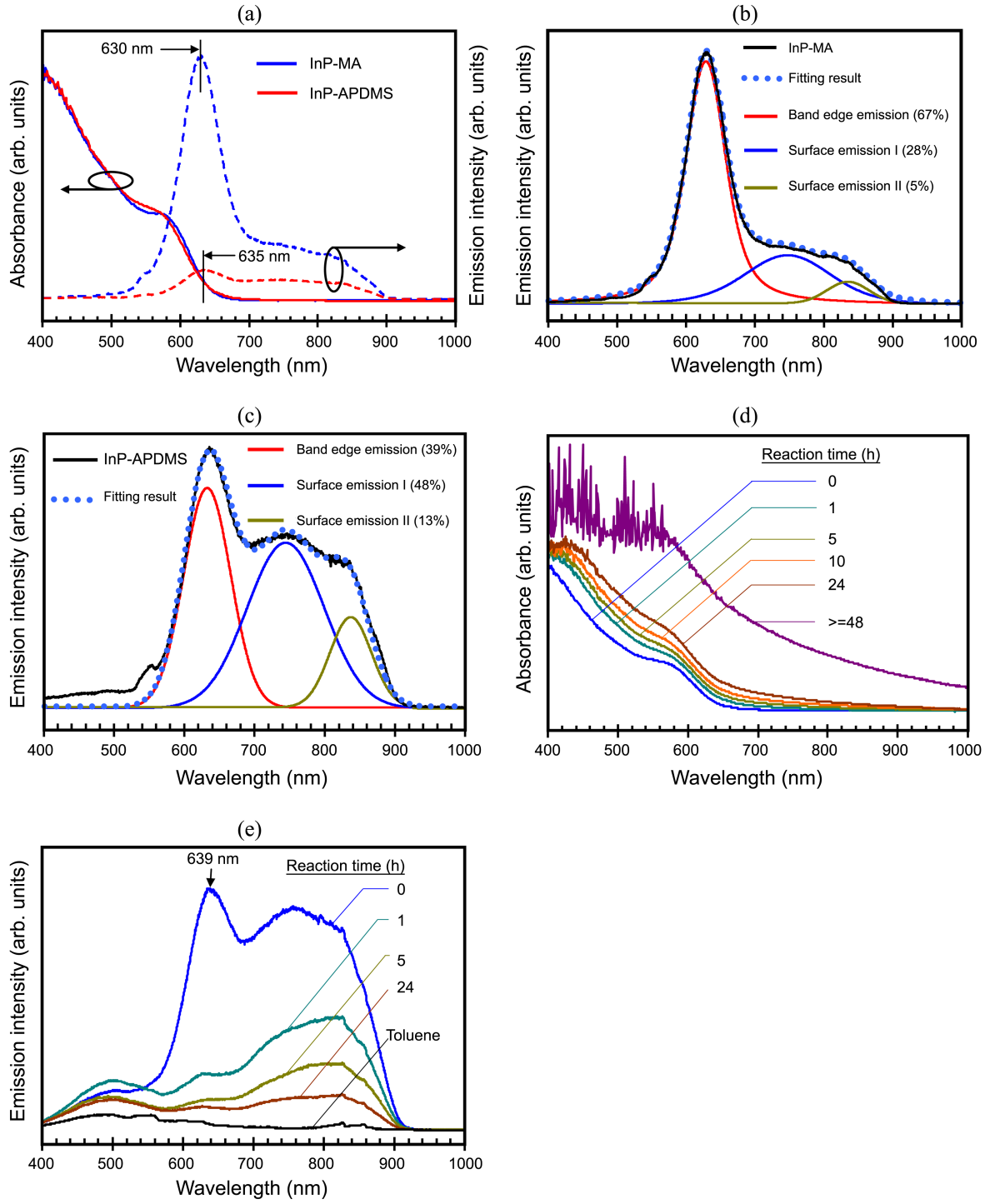

Figure 5. (a) UV absorbance (solid lines) and PL (dashed lines) spectra of the InP QDs solvated in toluene before (blue lines) and after (red lines) ligand exchange reaction with 3-aminopropyldimethylsilane. (b) Gaussian deconvoluted emission spectra of the InP-MA and (c) the InP-APDMS QDs. (d) UV absorbance and (e) PL spectra of the InP-organosilicon nanocomposite in toluene after various hydrosilylation reaction times.

Partial exchange of ligand from MA to APDMS does not significantly affect the UV absorbance of the InP QDs, but quenches the PL to about 10% of its original value and red-shifts the emission spectrum from 630 nm to 635 nm, as shown in Figure 5(a). After deconvoluting the emission spectra of InP-MA and InP-APDMS QDs using the Gaussian fitting method, as shown in Figure 5(b) and (c), respectively, we found that the relative contributions of the band and surface related emissions are changed in opposite ways. The band emission is quenched from 67% in the InP-MA QDs to 39% in the InP-APDMS QDs by the ligand exchange. These trends were also observed in the case of the InP/ZnS QDs, as shown in Figure 6(a) and Figure S4 (Supporting information). The PL intensity is also quenched to about 10% of its initial

value and the emission spectrum is red-shifted from 613 nm (InP/ZnS-MA QD) to 618 nm (InP/ZnS-APDMS QD). Concretely, the contribution of the band emission is decreased from 88% (in the InP/ZnS-MA QDs) to 62% (in the InP/ZnS-APDMS QDs) (Supporting information, Figure S4).

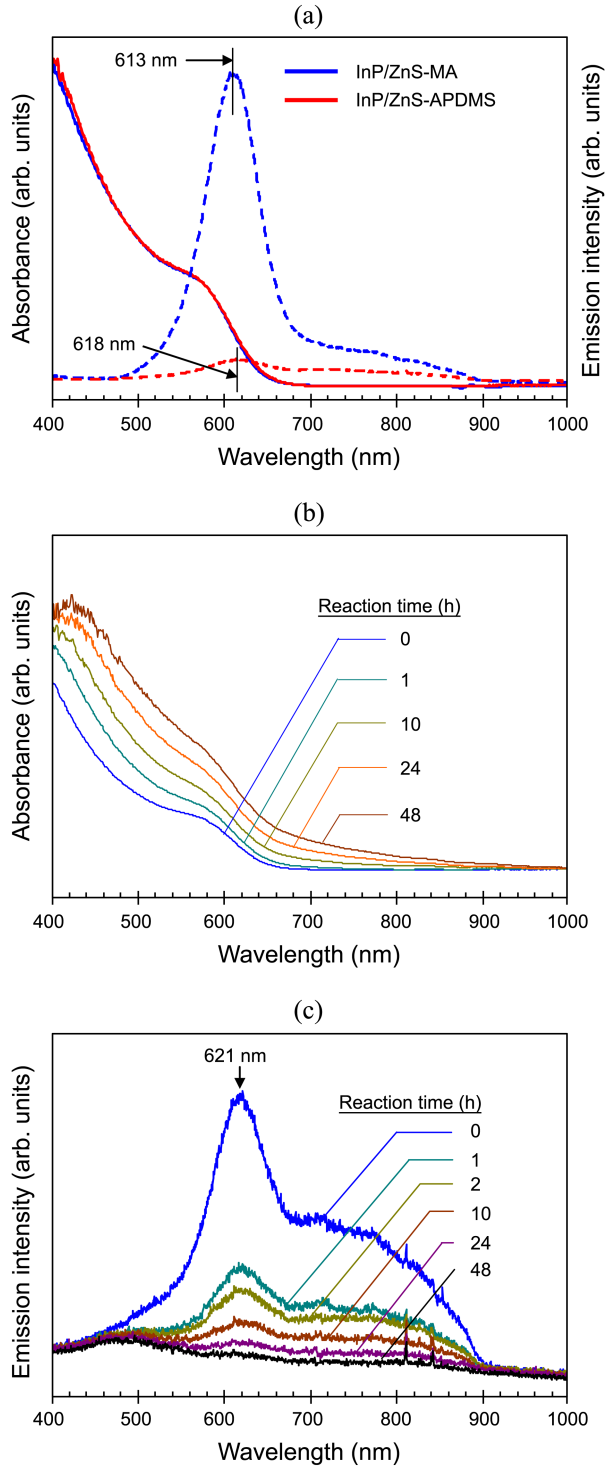

Figure 6. (a) UV absorbance (solid lines) and PL (dashed lines) spectra of the InP/ZnS QDs dispersed in toluene before (blue lines) and after (red lines) ligand exchange reaction with 3-aminopropyldimethylsilane. (b) UV absorbance and (c) PL spectra of the InP/ZnS QD-organosilicone nanocomposite in toluene solution after various hydrosilylation reaction times.

The PL quenching owing to the adsorption of APDMS, a small amine molecule, observed in our case is in contrast to the PL enhancement due to hexadecylamine (HDA) observed by S. Xu,[3] wherein the HDA added prior to the formation of InP QDs improves the surface passivation of the QDs, hence increases the PL. Additionally, addition of the HDA after the formation of InP QDs does not improve the PL.[3] R. Xie used a smaller amine, *n*-octylamine (OTA), to synthesize high quality InP QDs.[2a] These two contradicting effects of amine molecules on the PL of QDs have also been reported for CdSe QDs.[13a,b,c]

Herein, we address the three possible mechanisms which might be responsible for the changes in the emission spectra of the InP and InP/ZnS QDs due to ligand exchange with APDMS: 1) photoinduced hole transfer from the QD to the APDMS molecules, 2) non-radiative relaxation by energy transfer from the excited electrons to the adsorbed amine molecules, and 3) surface defects induced by the amine molecules having higher coordinating ability. These three mechanisms are conceptually modeled in Figure S5a, S5b (supporting information), and Figure 7, respectively.

The first mechanism, shown in Figure S5a, is not energetically favorable or discarded in our cases because the oxidation potential of APDMS of about 1.90 eV *vs.* NHE (with respect to a normal hydrogen electrode), assumed to be that of *n*-butylamine,[13a] is much higher than the valence band edge potential of the InP QDs of about 0.94 eV *vs.* NHE, fairly taken to be that of 3.6 nm InP QDs.[14] In the second mechanism, as shown in Figure S5b, the exciton can be distinguished in the QD-amine system by transferring the energy of the excited electron to various vibration modes of the amine molecules, resembling to a large molecular system, where the emission is reduced in intensity but unchanged in wavelength.[15] Therefore, we think that this mechanism is not working in our cases because it can not explain the red-shifts in the emission spectra, as previously mentioned in Figure 5(a) and 6(a).

Alternatively, we propose that the PL quenching due to

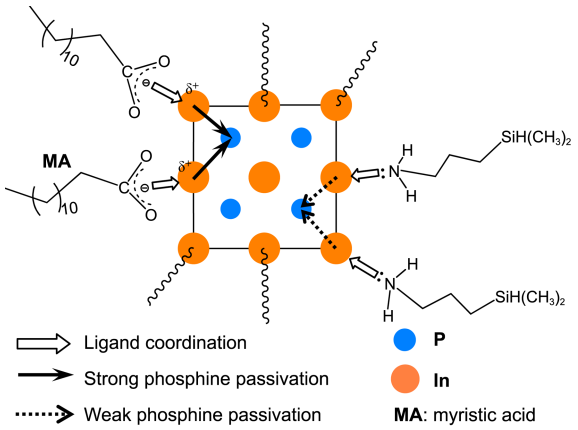

Figure 7. Ligand exchange induced surface defect mechanism: In this mechanism, the higher electron donating ability of APDMS gives rise to poorer phosphine passivation by weakening the In → P passivation.

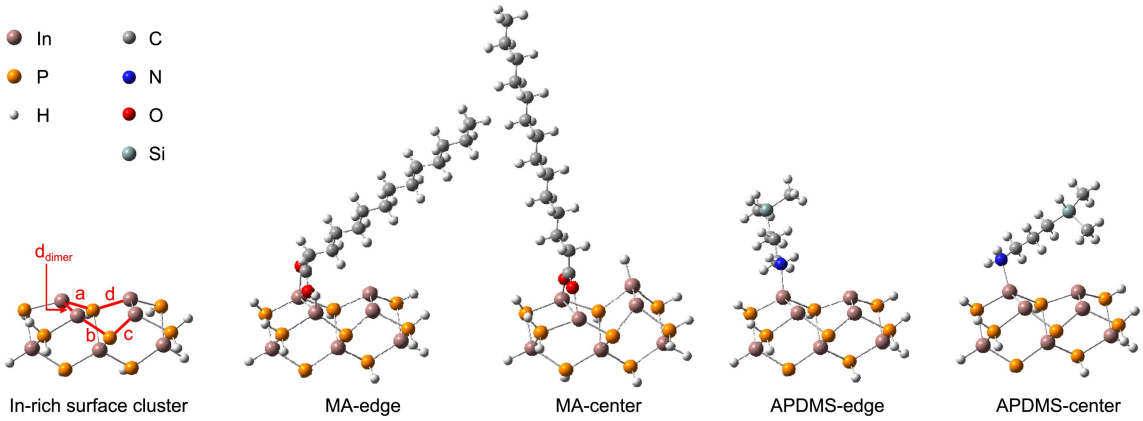

Figure 8. Optimized molecular structures of the indium-rich surface cluster and the MA- and APDMS-coordinated clusters. Bond lengths of interest are summarized in Table 2. The surface In-bulk P bonds denoted by a, and b are longer in the APDMS-coordinated cluster, indicating that replacing the MA ligand by the APDMS one weakens In → P passivation.

ligand exchange with APDMS originates from the increase in the number of surface states of non-metallic (P or S) atoms on the surface of the InP and InP/ZnS QDs. In this study, the InP QD was synthesized in an indium rich condition (In:P = 2:1) to generate excess indium atoms on the QD surface. The indium rich surface is to minimize the number of phosphine dangling bonds, so improves the PL efficiency.[3] Adding zinc to the surface of QDs was also reported to improve the PL efficiency by diminishing the number of phosphine dangling bonds.[3] While the indium or zinc atoms passivate the phosphine dangling bonds, represented by arrows in Figure 7, there exist unpassivated phosphine atoms having lone pair electrons (phosphine dangling bonds). Initially, the indium atoms on the surface of InP QDs are coordinated by the MA molecules. When the MA molecules are replaced by the stronger electron donating ligands such as APDMS or butylamine,[16] the indium atoms on the surface of InP-APDMS QDs are more stabilized, hence they have less tendency to accept electrons from their neighboring phosphine atoms than in the case of InP-MA QDs. Therefore, the stronger coordination of the indium atoms on the surface of the InP QD by APDMS induces the weaker indium to phosphine (In → P) passivation. Consequently, this poor passivation gives rise to two effects; 1) an increase in the number of phosphine dangling bonds, 2) the formation of surface electronic states near to the conduction band minimum of the QD due to the partially passivated phosphine atoms-we believe that the energy levels of the dangling bonds and surface electronic states are very different. The former explains the PL quenching after the ligand exchange, while the latter is regarded as the origin of the relative enhancement of the surface emission contributions observed in the case of the InP QDs, as shown in Figure 5(b) and c. In the case of the InP/ZnS QDs, in a similar way, the weaker passivation of the S and/or P atoms is also to be expected upon ligand exchange, accounting for the significant PL quenching and an increase in the surface emission contributions, as shown in Figure S4a and b.

The stronger passivation of the indium atom by a fatty amine than that afforded by carboxylic acid has been observed experimentally in the form of a reduction in the growing rate of the InP QD (emission wavelength vs. reaction time) when HDA was used together with carboxylic acid in the synthesis recipe.[17] As mentioned above, in this case, when the fatty amine is used prior the formation of the InP QD,[2a,3,17] the photoluminescence properties of the QD are improved or unaffected, in contrast to the PL quenching observed in our study when APDMS is used to replace the original carboxylic acid. We think this contrast in the PL changes is due to the fact that the poorly passivated phosphine resulted from the stronger ligand-metal coordination, as discussed above, can be compensated by reacting with other indium carboxylate complexes available in the reaction solution in the first case, but cannot be re-passivated in the post ligand exchange case. The better indium coordination obtained by using the amine while retaining the same degree of phosphine passivation explains why the PL of the InP QD is improved.[3]

To support our assertion that replacing the MA by the higher-electron donating ligand APDMS induces PL quenching by weakening the In → P passivation, theoretical calculations were carried out on a simple cluster model chemistry in Gaussian03[18a] (Supporting information, theoretical calculation). The change in the In → P passivation is investigated by considering the changes in the In-P bond lengths. Herein, the idealized In_7P_8 structure, as shown in the left side of Figure 8, was introduced to describe the indium rich InP QDs.[18b] Two situations that ligand molecule (MA or APDMS) is coordinated to the cluster by bonding to either one (edge form) or two (center form) surface indium atoms were both considered. The optimized structures of the whole cluster-ligand molecules and the interested In-P bond lengths are shown in Figure 8 and Table 2, respectively. From the bond lengths summarized in Table 2, it is obvious that replacing the MA ligand by the APDMS one lengthens the In-P bonds between the surface indium atoms and the bulk phosphine atoms, denoted by **a** and **b** in Figure 8. For example, the **a** bond is increased from 2.516 Å (*MA-edge*) or 2.489 Å (*MA-center*) to 2.612 Å (*APDMS-edge*) or 2.607 Å (*APDMS-center*), respectively. These increases prove to the previous conclusion that the exchange of ligand from MA to APDMS

Table 2. Calculated bond lengths (Å) in the indium-rich surface cluster and the MA- and APDMS-coordinated clusters. The coordination of the APDMS to the surface In atoms results in the longer surface In - bulk P bond lengths (**a**, **b**) compared to the MA case, implying that replacing the MA ligand by the APDMS one weakens the In → P passivation

	Cluster	MA-edge	MA-center	APDMS-edge	APDMS-center
a	2.562	2.516	2.489	2.612	2.607
b	2.533	2.539	2.440	2.548	2.547
c	2.533	2.503	2.667	2.518	2.517
d	2.562	2.608	2.724	2.574	2.577
$\mathbf{d}_{dimer}$	2.854	4.167	4.235	2.863	2.860

reduces the In → P passivation. The increases in the In-P bond lengths are in accordance with the previous mention that the higher electron donating ligand APDMS

The syntheses and characterizations of InP (InP/ZnS) QD-organosilicon nanocomposite materials, in which the QDs are in proximity were also performed in this study, in order to 1) investigate the origin of the physico-chemical interactions between the QDs which affect their optical properties and 2) design a basic process architecture for dispersing the QDs as a phosphor into the silicone encapsulants containing the vinyl-terminated silicone monomer for the white LED device.

Figure 5(d) and 6(b) show the UV absorption spectra of the reaction mixtures of the InP-APDMS and InP/ZnS-APDMS QDs with DVMSE in toluene solvent according to the hydrosilylation reaction time, respectively. As increasing the reaction time the absorbance in the long wavelength region (> 660 nm) increases and the onset point extends to the red side, while the excitonic peak becomes blurred without any significant red shift. We assert that this is due to the formation and growth of QD nanocomposites in which the QDs are cross-linked by the DVMSE molecules *via* hydrosilylation reactions. This argument is strongly supported by the scattering effect of the QD nanocomposites with a size of several tens of nanometers, as depicted in Figure 9(a). The individual QDs are too small to scatter light in the visible range, as clearly observed in the case of the InP-MA (InP/ZnS-MA) and InP-APDMS (InP/ZnS-APDMS) QDs in

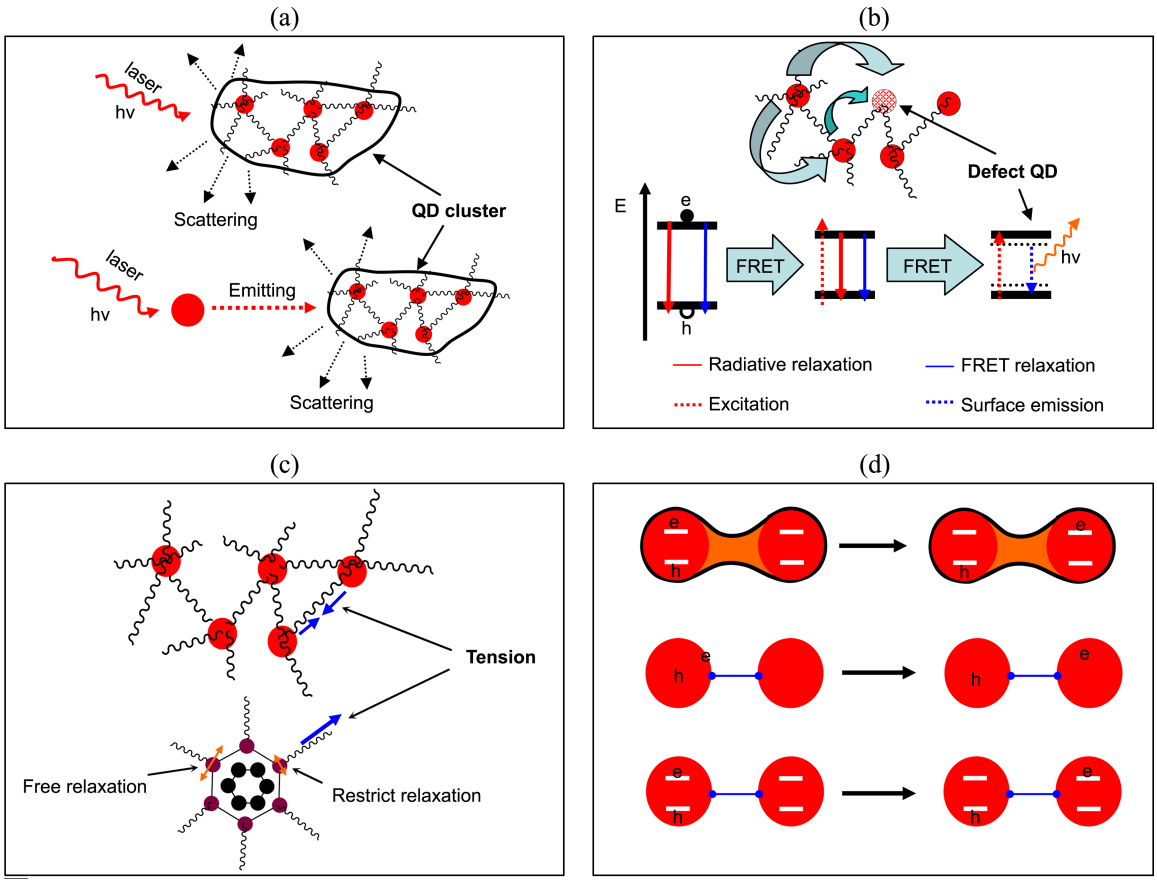

Figure 9. (a) PL quenching due to scattering effect originating from a large size QD-nanocomposite. The large size QD-nanocomposite can both scatter the incident laser so as to reduce the absorbance of the QDs (above) and scatter the light emitted from the excited quantum dot, thereby reducing the amount of light emitted from the sample. (b) FRET mechanism: within a QD-nanocomposite, one or multistep FRET concentrates the exciton energy onto the larger QDs and/or QDs with a surface defect, which shifts the emission to the red side and increases the contribution of the surface related emission. (c) Tension induced PL quenching mechanism: The tense linker restricts the relaxation of the atoms on the surface of the QD, thereby increasing the number of surface defects. d) Photoinduced charge (presented by electron) transfer mechanism: in the QD-nanocomposite (represented by coupled QDs) where the QDs are in the proximity, the exciton can be dissociated into the individual QDs *via* electronic coupling (first line), sequential tunneling of the trapped (second line) or core (third line) electrons.

Figure 5(a) and 6(a), respectively. However, the QD nanocomposites can cause a significant Rayleigh scattering effect, as illustrated by the scattering extinction α_{Scat} in Eq. (4) below, which contributes to the total UV absorption, in addition to the excitonic transition originating from the QDs.[19a] Here, α_{Scat}, V, λ, ρ, ε_{QD} and ε_{Sol} are the scattering extinction, volume confining the QD nanocomposite, wavelength, volume fraction of the QD nanocomposite, and the real parts of the dielectric functions of the QDs and solvent, respectively. As the QD nanocomposite grows (V increases), the scattering effect at wavelength λ, $\alpha_{Scat}(\lambda)$, increases, thereby increasing the overall UV absorbance.

$$\alpha_{scat} = \frac{4}{9} V \left(\frac{2\pi}{\lambda}\right)^4 \rho(1-\rho)(\varepsilon_{QD} - \varepsilon_{Sol})^2 \quad (4)$$

There is another important issue: the peak broadening and red shift which could be due to an enhancement in the dipole-dipole interaction within the QD ensembles,[20] or electronic coupling effect.[21] The former has been reported, however it broaden slightly the UV[20a] or FIR (far infrared) peaks and cause a very small red-shift (less than 1 nm).[20b] The latter effect is originated from the overlapping among the quantum dot electronic wavefunctions, which is both depending on the size of QD and the QD interdistance. The smaller quantum dots with shorter QD interdistances are in the QD assemble the more electronic coupling among the QDs is, and hence, the UV absorption peaks are more red shifted and broadened.[21] In our system, no evident red shift of the UV peak is observed, implying the absence of the electronic coupling effect. This is explained by the following two factors. The first one is that the electronic wavefunction is not likely to spread outside the large size InP QDs (red emitting QDs), as previously reported for the CdTe QDs system.[22] The second one is that the cross-linker, with a length of approximately 1.6 nm (Supporting information, Figure S6) is not short enough to lead to the hybridization of wavefunctions. Simply speaking, the electronic coupling effect can be ruled out for our QD-organosilicon nanocomposites. We assert that the Rayleigh scattering effect due to the formation and growth of QD nanocomposites is the origin of the peak broadening in the UV absorption spectra.

The physico-chemical interactions between the QDs in our QD-organosilicon nanocomposites can be understood more deeply by discussing the possible mechanisms explaining the PL quenching phenomena observed as the hydrosilyation reaction time is increased. As shown in Figure 5(e) and 6(c), respectively, the formation and growth of the QD-organosilicon nanocomposite shift the emission spectra to the red side and quench the PL in the InP and InP/ZnS QDs. As the size of the QD-composites is increased, with raising the reaction time, the intensity ratio between the surface related and band edge emissions is increased in the case of InP QD-composite but remained almost constant in the case of InP/ZnS-composite. We put forward here four possible mechanisms explaining these changes in the PL of the QD nanocomposites, namely 1) the effect of scattering, 2) Förster resonance energy transfer (FRET), 3) cross-linker tension and 4) photoinduced charge transfer, as modeled in Figure 9(a), (b), (c), and (d), respectively. The applicability of these mechanisms to the InP and InP/ZnS QD-organosilicon nanocomposites is summarized in Table 3, as will discussed in the following section.

Table 3. Possibilities of various PL quenching mechanisms being applied to the changes in the emission spectra of the InP and InP/ZnS QD-organosilicon nanocomposites

Mechanisms	InP QD nanocomposite	InP/ZnS QD nanocomposite
Scattering	**Accepted** - Increase in UV absorbance - Decrease in PL intensity	**Accepted** - Good UV transmittance - Decrease in PL intensity
FRET	**Accepted** - Red shift in PL - Increasing surface emission	**Accepted** - Slight red shift in PL
Cross-linker tension	**Accepted** - Decreasing PL	**Accepted** - Decreasing PL
Photoinduced charge transfer	**Excluded** - No QD coupling - Increasing surface emission	**Excluded** - No QD coupling - Surface emission not changed

In the first mechanism, as already discussed above about the absorbance peak broadening, the large size QD nanocomposites formed during the hydrosilylation reaction can scatter the incident laser light, thereby reduce the number of QDs being excited,[19b] as depicted in Figure 9(a). The decrease in the number of excited QDs results in a decrease in the total PL intensity. The QD nanocomposites can also scatter the light emitted from the QDs, so that the total light coming out of the sample is decreased.[19c] This scattering effect causes the observed overall PL intensity to be lower than that of the isolated QDs, regardless of their type. This effect is likely to have more effect on the samples at reaction times of 24 h (the InP QD case) and 48 h (InP/ZnS case), as already confirmed in the UV absorbance spectra, as shown in Figure 5(d) and 6(b), respectively.

The second mechanism, Förster resonance energy transfer (FRET) between the QDs, as depicted in Figure 9(b), is adopted in order to explain 1) the small red shift in the emission spectrum of the QD-organosilicon nanocomposite compared to the mother QD solutions 2) the increase in the contribution of the surface related emission with increasing reaction time, as shown in Figure 5(e). We firstly assume that the assembly of the QDs into the QD-organosilicon nanocomposite through hydrosilylation is QD size independent, so that the size distributions of the QD in the QD-composite and in the solution are the same. This is reasonable because Koole reported that the cross-linking efficiency of allylamine capped CdTe QDs with dithiol linkers is size independent.[23] Secondly, we assume that the edge-to-edge interdistance between the QDs in the QD-organosilicon nanocomposite is approximately equal to the distance between the two nitrogen atoms in the cross linker, *viz*. 1.6 nm, as estimated using a Gaussian calculation, (Supporting information, Figure S6). This short QD distance allows the energy of the exciton to be transferred from the smaller QD

(higher band gap) to the larger QD (lower band gap) within the QD-composite *via* the FRET mechanism.[24] FRET quenches the PL of the small QDs and enhances that of the larger ones. This is why the PL of the QD ensemble in the composite appears to be red shifted compared to that in the solution state, as shown in Figure 5(a) and 5(e), with the PL peak center being shifted from 635 nm (InP-APDMS) to 639 nm in the sample at reaction time = 0 h. In addition, in the case of the InP/ZnS QD, it is shifted from 618 nm (InP/ZnS-APDMS) to 621 nm, as shown in Figure 6(c). Note that since the samples were kept at about −20 °C and measured at room temperature, under these conditions the hydrosilylation reaction progressed slowly, so that the samples with a reaction time of 0 h can be regarded as solutions of the QD-nanocomposites.

In addition to the small red shift in the emission spectrum of the QD-nanocomposite compared to that in the QD solution, as discussed above, one obvious change in the emission spectrum of the InP-nanocomposite is that the contribution of the surface related emission increases with increasing reaction time, as shown in Figure 5(e). This can be understood based on the multistep FRET, which can also occur, especially in large QD-composites,[23] concentrating the exciton energy on a QD with surface electronic states-Note that the role of the surface electronic states was already proposed in Figure 5(a) and 6(a) to explain the relative enhancement of the surface related emission in the PL spectrum that appeared after ligand exchange with APDMS. As a result, the contribution of the surface related emission is increased at the cost of a decrease in the band emission.

In the case of the InP/ZnS QD, the number of surface electronic states is minimized by the passivation of the InP core by the higher band gap ZnS shell and, therefore, no significant increase in the surface related emission was observed, as shown in Figure 6(c).

The third mechanism, as depicted in Figure 9(c), is related to the tension induced by the cross linker on the surface of the InP QDs, which can be intuitively deduced from the so-called temperature antiquenching mechanism.[25a] As discussed earlier, the InP QDs are cross-linked in the QD-organosilicon nanocomposite by short linkers with a length of about 1.6 nm, which are placed in a state of tension by the QDs having large masses. The tensed linkers impart their stress to the surface of the QDs, so that the latter experience a rigid environment, which prevents their surface from undergoing free relaxation, as shown by the two headed arrows in Figure 9(c). The theoretical calculation shows that the unrelaxed CdSe QDs do not show luminescent behavior, because they have a continuous density of states (DOS) without a clear gap at the Fermi level.[26] The relaxed CdSe QDs, however, have an open gap and, therefore, exhibit luminescent behavior, since the number of midgap states originating from the dangling bonds is minimized by their undergoing a surface relaxation process.[26] Additionally, a capping agent such as trioctyl phosphine oxide (TOPO) attracts the Cd atoms on the surface of the CdSe QDs and displaces them from the stable state (fully relaxed state) by 0.15 Å.[26] In this case, the octyl tails of the TOPO molecules are fairly free, so that this small displacement does not affect the optical properties of the CdSe QDs. Although the calculation in the case where the tail of the capping agent is attracted by an external force has not been performed, we believe that the surface atoms would be displaced further from their relaxed states, resulting in more midgap states. Evidence supporting this hypothesis was demonstrated experimentally in a previous report, in which CdTe QDs were anchored in ice by cross-linkers of different lengths. The PL was slightly decreased in the case where the CdTe QDs were anchored by a long linker (less stress induced by the linker), but completely quenched in the case where a short linker (more stress) was used.[25b] Similarly, the restricted surface relaxation, as discussed above, probably results in "black" InP QDs, which do not have any luminescence at all, so that the total emission of the sample is decreased. Tension may also occur in the InP/ZnS-organosilicon nanocomposite, resulting in the quenching of the PL in a similar manner to the InP QD case, as shown in Figure 6(c). In addition, as discussed in the previous mechanism, where the exciton energy migrates in the QD-organosilicon nanocomposite through FRET or multistep FRET, the black QDs with a continuous DOS resulted from cross linker tension also quench the PL of the other QDs within the QD-nanocomposite.

Finally, we discuss the possibility of PL quenching by the formation of a separated electron-hole pair by photoinduced charge transfer from one QD to its neighbor within the QD-nanocomposite. There are two charge transfer mechanisms among the QDs: 1) electronic coupling where the electronic wave functions of the neighboring QDs overlap, forming a coherent molecular type orbital extended over many QDs, as depicted in the top row in Figure 9(d) and 2) sequential tunneling where the coupling between neighboring QDs is weak and their electronic wave functions are still identical, as depicted in the middle and bottom rows in Figure 9(d).[27a] As discussed previously, the UV peaks of the QD-organosilicon nanocomposite are not red shifted compared to those of the individual quantum dots, as shown in Figure 5(d) and 6(b), indicating that the QDs are not electronically coupled in the QD-nanocomposite. Therefore, the first charge transfer mechanism can be ruled out in our case, *viz.* the InP and InP/ZnS QD-organosilicon nanocomposites. At this moment, we need to consider the possibility of the second charge transfer mechanism. We mentioned earlier that the InP-APDMS and InP/ZnS-APDMS QDs show a considerable surface related emission, indicating that the excited electrons are transferred to the surface electronic states of the QDs. Since the electrons trapped in the surface states have less Coulombic attraction with the excited holes compared to the electrons in the conduction band, less energy is required for tunneling to the neighboring QDs (shown in the middle row in Figure 9(d)) than that for band electron tunneling (shown in the bottom row in Figure 9(d)).[27b] As a result, if charge transfer occurred in the QD-organosilicon nanocomposites, the population of trapped electrons (electrons in the surface

electronic state) would be decreased or the contribution of the surface related emission to the total emission spectrum would decrease. Herein, however, we observed that the contribution of the surface related emission increases with increasing reaction time in the InP-organosilicon nanocomposite, as shown in Figure 5(e). Therefore, we can exclude the possibility that the PL is quenched by the charge transfer mechanism in the InP-organosilicon nanocomposite. In the case of the InP/ZnS-nanocomposite, although we did not observe the trend in the surface related emission, we can also exclude the possibility of charge transfer between the InP/ZnS QDs, because of the fact that the tunneling energy cost is increased by their wider band gap ZnS shell.[27b]

Conclusion

We designed a new capping agent, 3-aminopropyldimethylsilane, which has the Si-H functional group, to overcome the self-condensation problem and be able to combine chemically with the silicone encapsulant through the hydrosilylation reaction. The use of the new ligand overcame the incompatibility problem between the QDs, which are mostly capped by fatty ligand and silicone encapsulants. The ligand exchange from MA to APDMS does not significantly affect the UV absorbance of the InP QDs, but quenches the PL to about 10% of its original value with the relative increase in surface related emission intensities. This is explained by stronger coordination of APDMS to the indium atoms on the surface of the InP QD, inducing 1) the increase in the number of phosphine dangling bonds, 2) the formation of surface electronic states near to the conduction band minimum of the QD, which is supported by longer bond length between the surface In atom and bulk P atom estimated in the cluster model calculations using DFT-B3LYP level. The interaction between the QDs was also investigated in the QD-organosilicon nanocomposite material where the QDs are cross-linked by a short linker, 1,4-tetramethydivinylsilylethane. Further PL quenching was observed in both the InP and InP/ZnS QDs when they formed the composites. We assert that there are three possible mechanisms explaining the PL quenching of the QD nanocomposites, namely, (1) the effect of scattering, (2) Förster resonance energy transfer (FRET), and (3) cross-linker tension.

Acknowledgments. This research was supported by the Basic Science Research Program through the National Research Foundation of Korea (NRF) funded by the Ministry of Education, Science and Technology (No. 2010-0008824). This work was also supported by the PLSI supercomputing resources of KISTI (Korea Institute of Science and Technology Information). Following are results of a study on the "Human Resource Development Center for Economic Region Leading Industry" Project, suppported by the Ministry of Education, Science & Technology (MEST) and the National Research Foundation of Korea (NRF).

Supporting Information Available. The synthesis of the APDMS ligand, physical and chemical mixing procedures, theoretical, Fig. S1 (a) GS-MS spectrum, Fig. S1 (b) ^{1}H-NMR spectrum, Figure S2. (a) Wide angle X-ray diffraction pattern and Figure S2. (b) TEM picture of the InP-MA QD, Figure S3. ^{13}C-NMR spectra, Figure S4. (a) Gaussian deconvoluted emission spectrum of the InP/ZnS-MA, and Figure S4. (b) InP/ZnS-APDMS, Figure S5. (a) Photoinduced hole transfer mechanism, Figure S5. (b) Fast electron thermalization mechanism. Figure S6. Geometric optimization of the linker, and Complete author list of reference 18a. are available free of charge *via* the internet at: http://journal.kcsnet.or.kr/.

References

1. (a) Mcguire, J. A.; Joo, J.; Pietryga, R. M.; Schaller, R. D.; Klimov, V. I. *Acc. Chem. Res*. **2008**, *41*, 1810. (b) Dai, Q.; Duty, C. E.; Hu, M. Z. *Small* **2010**, *6*, 1577.
2. (a) Xie, R.; Battaglia, D.; Peng, X. *J. Am. Chem. Soc*. **2007**, *129*, 15432. (b) Battaglia, D.; Peng, X. *Nano Lett*. **2002**, *2*, 1027. (c) Li, L.; Protière.; Reiss, P. *Chem. Mater*. **2008**, *20*, 2621. (d) Su, H.; Xu, H.; Gao, S.; Dixon, J. D.; Aguilar, Z. P.; Wang, A. Y.; Xu, J.; Wang, J. *Nanoscale Res. Lett*. **2010**, *5*, 625. (e) Baek, Jinyoung.; Allen, P. M.; Bawendi, M. G.; Jensen, K. F. *Angew. Chem. Int. Ed.* **2011**, *50*, 627. (f) Li, L.; Reiss, P. *J. Am. Chem. Soc*. **2008**, *130*, 11588.
3. Xi, S.; Ziegler, J.; Nann, T. *J. Mater. Chem.* **2008**, *18*, 2653.
4. (a) Wang, X.; Ren, X.; Kahen, K.; Hahn, E. A.; Rajeswaran, M.; Zacher-M, S.; Silcox, J.; Cragg, G. E.; Efros, A. L.; Krass, T. D. *Nature* **2009**, *459*, 686. (b) Nie, S.; Smith, A. M. *Nat. Biotechnol.* **2009**, *27*, 732.
5. (a) Schlotter, S.; Schmidt, R.; Schneider, J. *Apll. Phys. A* **1997**, *64*, 417. (b) Narukawa, Y. White-light LEDs. *Opt. Photonics News* **2004**, *15*(4), 24.
6. (a) Schubert, E. F. *Light-Emitting Diodes*, 2nd ed.; Cambridge University Press: New York, 2006. (b) Norris, A. W.; Bahadur, M.; Yoshitake, M. *Proc. of SPIE*. **2005**, *5941*, 594115-1. (c) Choi, J. K.; Lee, D.-H.; Rhee, S. K.; Jeong, H. D. *J. Phys. Chem. C* **2010**, *114*, 14233.
7. (a) Schreuder, A. M.; Gosnell, D. J.; Smith, J. N.; Warnement, R. M.; Weiss, M. S.; Rosenthal, J. S. *J. Mater. Chem.* **2008**, *18*, 970. (b) Barton, A. F. M. *CRC Handbook of Polymer-Liquid Interaction Parameters and Solubility Parameters*; CRC Press, Inc: Florida, 1990.
8. Gagneux, A. C.; Delpech, F.; Nayral, C.; Cornejo, A.; Coppel, Y.; Chaudret, B. *J. Am. Chem. Soc.* **2010**, *132*, 18147.
9. Li, C.; Ando, M.; Enomoto, H.; Murase, N. *J. Phys. Chem. C* **2008**, *112*, 20190.
10. Ziegler, J.; Xu, S.; Kucur, E.; Meister, F.; Batentschuk, M.; Gindele, F.; Nann, T. *Adv. Mater.* **2008**, *20*, 4068.
11. Lafaurie, A.; Azema, N.; Ferry, L.; Cuesta-L, J. *Powder Technol.* **2009**, *192*, 92.
12. Kuno, M.; Lee, J. K.; Dabbousi, B. O.; Mikulec, F. V.; Bawendi, M. G. *J. Chem. Phys.* **1997**, *106*, 9869.
13. (a) Sharma, S. N.; Shrma, H.; Singh, G.; Shivaprasad, S. M. *Mater. Chem. Phys.* **2008**, *110*, 471. (b) Landes, C. F.; Braun, M.; El-Sayed, M. A. *J. Phys. Chem. B* **2001**, *105*, 10554. (c) Landes, C.; Burda, C.; El-Sayed, M. A. *J. Phys. Chem. B* **2001**, *105*, 2981.
14. Blackburn, J. L.; Selmarten, D. C.; Ellingson, R. J.; Jones, M.; Micic, O.; Nozik, A. J. *J. Phys. Chem B* **2005**, *109*, 2625.
15. Darugar, Q.; Landes, C.; Link, S.; Schill, A.; El-Sayed, M. A. *Chem. Phys. Lett.* **2003**, *373*, 284-291.
16. McCafferty, E. *Introduction to Corrosion Science*; Springer: New York, 2010; p 364.
17. Xu, S.; Klama, F.; Ueckermann, H.; Hoogewerff, J.; Clayden, N.; Nann,T. *Sci. Adv. Mater*. **2009**, *1*, 125.

18. (a) Frisch, M. J.; *Gaussian03*; Gaussian, Inc.: Wallingford, CT, 2005. (b) Raghavachari, K.; Fu, Q.; Chen, G.; Li, L.; Li, C. H.; Law, D. C.; Hicks, R. F. *J. Am. Chem. Soc.* **2002**, *124*, 15119.
19. (a) Filonovich, S. A.; Rakovich, Y. P.; Vasilevskiy, M. I.; Artemyev, M. V.; Talapin, D. V.; Logach, A. L.; Rolo, A. G.; Gomes, M. J. M. *Monatsh. Chem.* **2002**, *133*, 909. (b) Ishii, S.; Ueji, R.; Nakanishi, S.; Yoshida, Y.; Nagata, H.; Itoh, T.; Ishikawa, M.; Biju, V. *J. Photochem. Photobio. A* **2006**, *183*, 285. (c) Müller, M. G.; Georgakoudi, I.; Zhang, Q.; Wu, J.; Feld, M. S. *Appl. Opt.* **2001**, *40*, 4633.
20. (a) Boev, V. I.; Filonovich, S. A.; Vasilevskiy, M. I.; Silva, C. J.; Gomes, M. J. M.; Talapin, D. V.; Rogach, A. L. *Physica B* **2003**, *338*, 347. (b) Vasilevskiy, M. I.; Rolo, A. G.; Artemyev, M. V.; Filonovich, S. A.; Gomes, M. J. M.; Rakovich, Y. P. *Phys. Status Solidi B* **2001**, *224*, 599.
21. (a) Mićić, O. I.; Ahrenkiel, S. P.; Nozik, A. J. *Appl. Phys. Lett.* **2001**, *78*, 4022. (b) Lazarenkova, O. L.; Banlandin, A. A. *J. Appl. Phys.* **2001**, *89*, 5509.
22. Koole, R.; Liljeroth, P.; Donega, C. M.; Vanmaekelbergh, D.; Meijerink, A. *J. Am. Chem. Soc.* **2006**, *128*, 10436.
23. Koole, R.; Luigjes, B.; Tachiya, M.; Pool, R.; Vlugt, T. J. H.; de Mello Donegá, C.; Meijerink, A.; Vanmaekelbergh, D. *J. Phys. Chem. C* **2007**, *111*, 11208.
24. Rogach, A. L. *Semiconductor Nanocrystal Quantum Dots: Synthesis, Assembly, Spectroscopy and Applications*; Springer Wien New York: Wien, 2008; p 277-310.
25. (a) Wuister, S. F.; Houselt, A. V.; Donegá, C. D. M.; Vanmaekelbergh, D.; Meijerink, A. *Angew. Chem.* **2004**, *116*, 3091. (b) Wuister, S.; Donegá, C. D. M.; Meijerink, A. *J. Am. Chem. Soc.* **2004**, *126*, 10397.
26. Puzder, A.; Williamson, A. J.; Gygi, F.; Galli, G. *Phys. Rev. Lett.* **2004**, *92*, 217401.
27. (a) Talapin, D. V.; Lee, J.-S.; Kovalenko, M. V.; Shevchenko, E. V. *Chem. Rev.* **2010**, *110*, 389. (b) Leatherdale, C. A.; Kagan, C. R.; Morgan, N. Y.; Empedocles, S. A.; Kastner, M. A.; Bawendi, M. G. *Chem. Rev. B* **2000**, *62*, 2669.